PS/OP/Note 90-4
17.1.1990

The PS Cycle for LEAR

Steve Hancock

Preamble

This document is not intended as an exhaustive reference. It aims, instead, to provide some physical insight into how the LEA cycle of the PS came to have its present design. The theoretical considerations which constrain the parameters involved in each of the operations comprising the cycle are discussed, but laborious derivations are avoided. In addition, some technical details which remain hidden at the level of the consoles are "exposed". It is hoped that this note will promote a greater understanding of the various features of the cycle which, together with the complementary reference log diligently compiled by Claude Saulnier, will make troubleshooting easier for the operations crews.

Préambule

Le présent document ne prétend pas à l'exhaustivité. Il vise plutôt à donner un aperçu des justifications physiques de la conception actuelle du cycle LEA du PS. Les considérations théoriques qui limitent les paramètres de chacune des opérations composant le cycle sont discutées, mais les développements fastidieux quant à leur origine évités. En outre, certains détails techniques qui restent cachés au niveau des consoles sont dévoilés. L'auteur espère que cette note permettra de mieux comprendre les diverses caractéristiques du cycle, ce qui, avec la liste des références diligemment établie par Claude Saulnier, facilitera le diagnostic des pannes par les équipes chargées de l'exploitation.

Contents

1. INTRODUCTION

1.1 Purpose

The rôle of the LEA cycle is to supply a single bunch of antiprotons at a momentum $p = 0.609$ GeV/c ($T = 180$ MeV) to the Low-Energy Antiproton Ring.

The rather curious value of the momentum at extraction from the PS derives from several considerations, some of them historical. The principal constraint is the lower limit of the frequency that can be maintained by the RF cavities of the PS. In the absence of any radial perturbation, this is given by

$$f_{RF} = \frac{hc}{2\pi R_{nom}}\left[1+\left(\frac{m_0 c}{p}\right)^2\right]^{-1/2} \geq 2.6\ \text{MHz}\,, \qquad (1.1)$$

where $m_0c = 0.938$ GeV/c for antiprotons (and protons) and $R_{nom} = 100$ m. The antiprotons are provided by the Antiproton Accumulator at $p = 3.575$ GeV/c, which immediately implies a harmonic number $h > 5.6$ in order to inject them into the PS. Now the circumference of LEAR is only one eighth of that of the PS, which, assuming comparable RF voltages, would suggest $h = 8$ for a matched bunch-to-bucket transfer between the two machines ($h_{LEAR} = 1$). However, the PS normally operates using $h = 20$ so that the change in the relative phasing of the RF cavities becomes more straightforward with $h = 10 \Rightarrow p \geq 0.609$ GeV/c.

Thus the PS provides a doorway between the AA and LEAR by decelerating antiprotons as far as it can on a convenient harmonic.

1.2 Characteristics of the LEA Beam

The LEA cycle is a low-energy, low-intensity one and, as such, involves no longitudinal emittance blow-ups and no octupole or poleface winding fields. Indeed, the skew quadrupoles are the only correction elements employed during the cycle; the trim dipoles, (normal) quadrupoles and sextupoles are all disabled. Thus the LEA beam sees the "bare machine", save for the skew quadrupoles which compensate for the coupling between horizontal and vertical transverse motion introduced, at very low energies, by the earth's own magnetic field.

The beam is below transition throughout the cycle.

The characteristics of the beam delivered to LEAR are, to some extent, governed by what is unstacked from the AA. The principal ones are summarized in the following table.

Momentum	0.609 GeV/c
Intensity	$\leq 2\times10^{10}$ antiprotons in 1 bunch
Longitudinal Emittance	~ 0.08 eV.s
Bunch Length	~ 100 ns
Normalised Transverse Emittances	< 8 π.mm.mrad (in both planes)

2. PLS PROGRAMME

Although the LEA cycle is a low-energy one, the user LEA (PLS line 40) is constructed from a combination of PLS lines which includes so-called high-energy operations. This is merely convention.

The complete list of entries in the PS user matrix is given below.

	LEA	PLS Line
Cycle Type	D	44
Harmonic Number	10	53
LE Working Point	LEDEC	60
HE Working Point	NOHE	70
Particle Type	ANTIP	74
"HE" Operation 16	FI16A	6
"HE" Operation 58/62/26	FE26	14
Linac Destination	.....	
Simulation (Y/N)	N	
Ejection 58 Destination	-	
Internal Dump	-	
"Ejection 16 Destination"	ATPA	30
PBAR/-	PBAR	17
Miscellaneous	-	
Dump 48 Timing	0	
Dump 47 Timing	0	

The terms in inverted commas are misnomers for the LEA cycle.

3. MAGNETIC CYCLE

The D cycle is unique in the arsenal of PS magnetic cycles in that it affords the deceleration of particles. In addition to the LEA cycle, it may be used to decelerate protons down to T~50 MeV (user TST, h=20) in order to investigate the low-energy closed orbit of the PS. Since the suppression of direct injection from the linac, this possibility has no operational consequences for the machine, but it does mean that the D cycle has a magnetic ledge for injection from the PS Booster as well as one at a field corresponding to 3.5 GeV/c. (In fact, this feature is common to most PS magnetic cycles.)

D cycle number 66 has an injection ledge of 804 Gauss, corresponding to T = 1 GeV, while D cycle number 65 was used for 815 MeV injection and is now redundant. Details of the former are illustrated in Figure 3.1. Both are 1.2 s cycles, which is the basic period of the Linac Beams Sequencer.

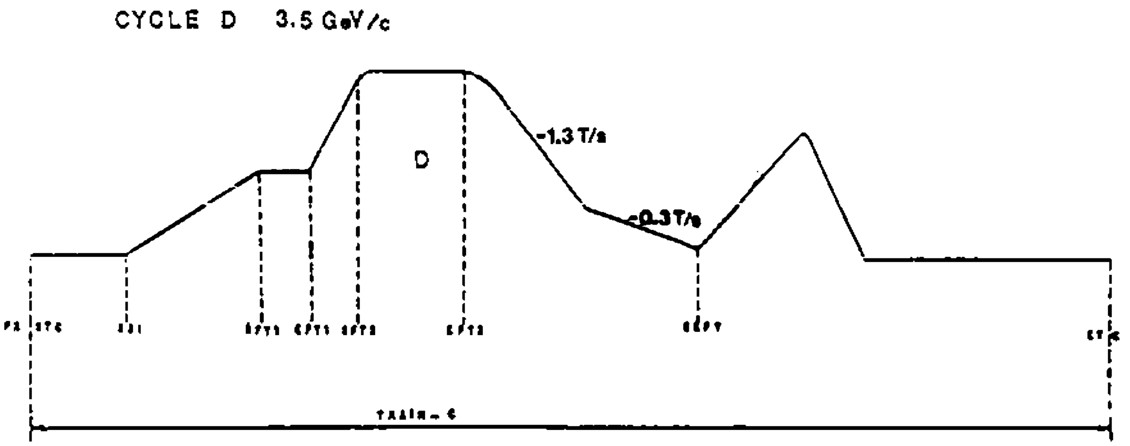

NO	FIX POINT		T/INTERV.MSEC
1	STC	-C1	1.00
2	STC	-SBI	100.00
3	ETC	-STC	30.00
4	SBI	-SFT1	111.00
5	SFT1	-EFT1	20.00
6	EFT1	-EBI	76.00
7	EBI	-SFT3	1.00
8	SFT3	-EFT3	136.00
9	EFT3	-SLFT	98.00
10	SLFT	-ELFT	101.00
11	ELFT	-EPC	4.09
12	EPC	-ETC	522.91
13	SBI	-SBD	10.58
14	SBI	-SBF	10.52
15	SBI	-SFP	16.90
16	SBI	-SRF800	
17	SBD	-SFP	— 6.33
18	SBD	-SRF800	
19	FKFA45	-WTR	14.00
20	FPC	-STC	600.01

CYCLE TYPE : D NO: 66
INJECTION :1.688 GEV/C
REPEAT.TIME : 1.2 SEC.
MAX.MOMENTUM : 3.43 GEV/C

CORRELATION			
NO		C	B1
1	SBD	111	53.9
2	SBF	111	53.9
3	SFP	117	110.8
4	SFT1	211	804.1
5	WTR	215	804.1
6	EFT1	231	803.8
7	SFT3	308	1637
8	EFT3	444	1690.3
9	SLFT	542	512.9
10	ELFT	643	146.8

Figure 3.1: The PS magnetic cycle for LEAR.

The D cycle has no ejection ledge. Instead, the ejection process is triggered by a specified value of the B-field itself. For this reason, ejection occurs during the second phase of the deceleration when the magnetic field is changing by only -3 Gauss per millisecond ($dp/dt = -6.3$ MeV/c/ms). The bulk of the deceleration is achieved during the first phase, during which $dB/dt = -1.3\ T.s^{-1}$ ($dp/dt = -27$ GeV/c/s). The main magnet power supply cannot turn off properly, however, if the slope of the field is insufficiently steep. Consequently, after ejection, the field is ramped back up before being brought down to zero at a higher rate.

4. INJECTION

4.1 Overview

The operation FI16A for the injection into the PS of antiprotons for LEAR is identical to that of the SPN, h = 6 + 12 cycle which supplies antiprotons to the SPS collider. Indeed, an h = 6 RF train is distributed for the fine injection timing of both cycles irrespective of the fact that, in the case of the LEA cycle, the beam is captured on h = 10.

The injection of a single bunch of antiprotons is achieved via a pulsed magnetic septum in straight section 16. The closed orbit in this region is deformed by dipoles PR.DHZ12, 14, 20 and 22, which constitute the 4-bump BSW16LE. With four dipoles it would be possible to control both the position and the angle of the closed orbit at the septum without perturbing the orbit elsewhere around the machine. In practice, however, the four dipoles are not powered independently but in series, so that the angle at the septum is determined by the choice of bump amplitude. Nevertheless, since the bump is centred on straight section 17, there remains a non-zero angle at the septum which favours injection. Normalized transverse phase space and real space representations of slow bump BSW16LE are shown in figure Figure 4.1. Only two modules of the full-aperture kicker PR.KFA79 are required to complete the injection process.

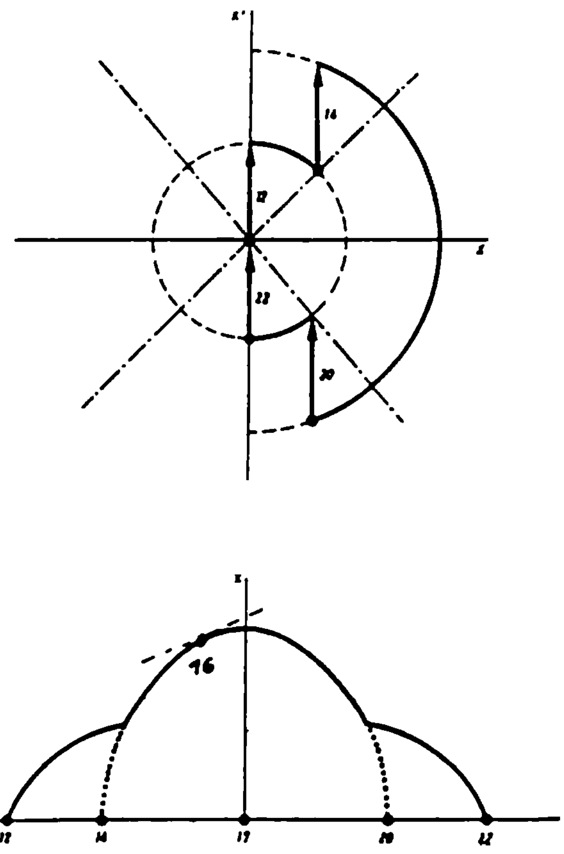

Figure 4.1

The injection optics are normally adjusted by means of the TST proton beam, but coherent transverse antiproton oscillations provoked by any residual errors are, anyway, damped during the first few hundred microseconds after injection by a transverse feedback ("damper") system working in both planes.

4.2 RF Synchronization

The h = 10 low-level RF beam control is, perhaps, the simplest in the Central Building. It relies upon a synthesized revolution frequency generator whose output is multiplied by ten by a phase-locked loop to produce the RF frequency that drives the cavities. The only feedback loop employs wide-band pick-up 13 to provide the beam phase information (filtered at the revolution frequency) that is used to correct the phase and frequency of the output of the PLL. The design is dominated by the need to cope with the large frequency swing during deceleration and, consequently, features an additional "fast" (ac-coupled) branch of the phase loop which can modify the PLL frequency in competition with the synthesizer. The phase loop operates at the revolution frequency so that the pick-up signal derived from a low-intensity beam is not masked by direct RF coupling from the cavities themselves.

A couple of milliseconds before injection (timing PX.SDFR10), when there is no beam information, an RF signal derived from the AA cavity that unstacks the antiprotons is divided by four and used instead. This enables the PS to synchronize onto the nominally-correct revolution frequency to receive particles from a machine that is a quarter of its size. A few turns after injection (timing PX.SSW3.5GEH10), to allow for the filling time of filters, etc., the so-called 3.5 GeV/c injection switch switches back to pick-up 13, closing the phase loop on the beam.

If the dipole magnetic field on the 3.5 GeV/c ledge is incorrect, the injected antiproton bunch will still circulate at the nominal frequency, but not on the central orbit. Then, when the phase loop closes, its "slow" branch will enable the synthesizer gradually to impose the RF frequency that is appropriate to the erroneous field and the beam will become centred in the machine.

5. EJECTION

5.1 Overview

The fast extraction of the beam towards LEAR is achieved very simply with a single kicker module mounted outside the vacuum chamber in straight section 28 and a pulsed magnetic septum in straight section 26. There are no closed orbit bumps and no kick enhancement quadrupoles involved in this operation.

KFA28 produces an angular deflection $\Delta x'$ which translates, two straight sections downstream, into a horizontal displacement given by

$$\Delta x = \beta_H^{(28)} \Delta x' \sin\Delta\psi ,$$

where $\beta_H^{(28)} = 12.6$ m and the betatron phase advance over the two straight sections is $\Delta\psi \simeq \pi/4$. This result follows directly from normalised transverse phase space ("circle diagram") considerations. Since the beam is some 50 mm wide at ejection, a jump of $\Delta x > 80$ mm is required to clear the 3 mm blade of SMH26 which is located 53 mm from the centre of the vacuum chamber. This implies that

$\Delta x' > 9$ mrad or, since (for small $\Delta x'$)

$$\Delta x' \text{ [mrad]} = \frac{1}{33.356p \text{ [GeV/c]}} \int B.dl \text{ [Gauss.m]} ,$$

that the required magnetic length of KFA28 is ~200 Gauss.m. In practice this is achieved with a charging voltage of ~30 kV.

The kicker and septum voltage pulses are both shown in Figure 5.1. Due to the low extraction momentum, SMH26 is not a particularly high-power device and this simplifies the circuit design of its power supply since it is not necessary to "clip" the resonant discharge after the first half sine wave.

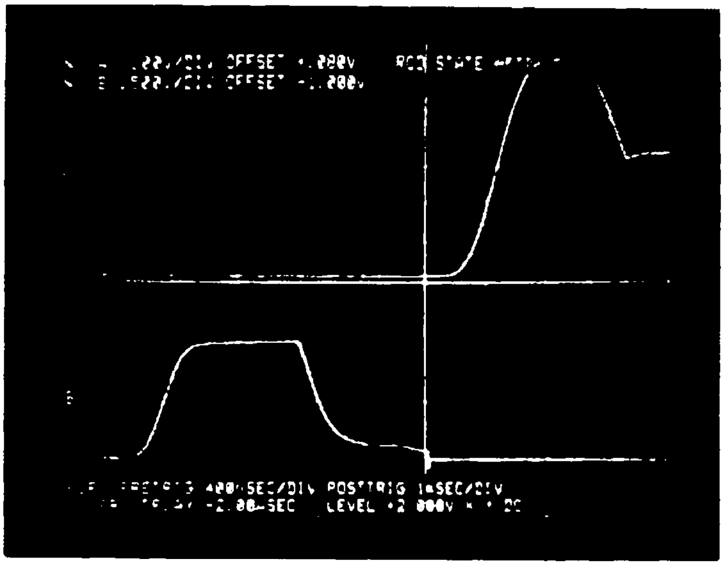

Figure 5.1: SMH26 (channel A) and KFA28 (channel B) pulse shapes seen on a split timebase oscilloscope triggered by the timing pulse PX.O26 delayed 8 μs. (The kicker pulse is somewhat degraded by the ~20 MHz bandwidth of the Signals Observation System.)

5.2 RF Synchronization

Since the LEAR machine is empty prior to extraction from the PS, it is the job of the LEAR cavities to synchronize onto those of the PS. The process is, therefore, transparent from the point of view of the PS machine.

5.3 Influence of the B-train on Ejection Stability

The coarse timing which initiates the ejection process is derived from the B-train (see section 7). Consequently, any variation of the B-train with respect to the true magnetic field will cause the energy of the extracted beam to fluctuate. Furthermore, since there is no radial loop in the h = 10 low-level RF beam control, any difference between the B-train and the dipole field will also produce a radial displacement of the beam at the moment of ejection. This is because the synthesized decelerating RF is a function of the B-train:

$$f_{RF} = \frac{hc}{2\pi R_{nom}}\left[1+\left(\frac{m_0 c}{eB_{meas}\rho_{nom}}\right)^2\right]^{-1/2} \tag{5.1}$$

(Cf. equation (1.1).) Here, e is the magnitude of the charge on the antiproton, B_{meas} is the measured field value obtained by counting B-train pulses and $\rho_{nom} = 70.079$ m is the nominal bending radius.

In order to estimate the effect of an error in $B_{meas} = B + \Delta B$, we substitute for $f_{RF} = hf_{rev}$ in equation (5.1) using $f_{rev} = \beta c/2\pi R$, where βc is the speed of the antiprotons and $R = R_{nom} + \Delta R$ is their mean radius. This yields

$$\frac{R}{R_{nom}} = \beta\left[1+\left(\frac{m_0 c}{eB_{meas}\rho_{nom}}\right)^2\right]^{-1/2} \tag{5.2}$$

Now, the fundamental guide field relation is

$$p = eB\rho_{nom}\left(\frac{R}{R_{nom}}\right)^{\gamma_{tr}^2}, \tag{5.3}$$

where $p = m_0\beta\gamma c$ and $\gamma_{tr} \simeq \sqrt{37}$ is the value of $\gamma = (1-\beta^2)^{-1/2}$ at transition in the PS. Hence

$$\beta = \left\{1+\left[\frac{eB\rho_{nom}}{m_0 c}\left(\frac{R}{R_{nom}}\right)^{\gamma_{tr}^2}\right]^{-2}\right\}^{-1/2} \tag{5.4}$$

Equations (5.2) and (5.4) together yield a non-linear expression in R/R_{nom} which may be solved numerically.

For example, suppose that the B-train field measurement is 1 Gauss higher than the true field, B. The theoretically correct value of the field at ejection, $B_{ej} = 0.029$ T, is obtained by putting $p = 0.609$ GeV/c and $R = R_{nom}$ into equation (5.3). However, since ejection is triggered when $B_{meas} = B_{ej} \Rightarrow B = B_{ej} - \Delta B$, the actual field at ejection will be 1 Gauss lower than the correct value. Under these conditions, the numerical solution for R/R_{nom} gives the radial displacement at ejection as

$$\Delta R = +9.7\ \text{mm} \qquad [\Delta B = +1\ \text{Gauss}]$$

This radial position error produces a contribution to the momentum error which cancels, to some extent, that due to the incorrect field:

$$\frac{\Delta p}{p} = \gamma_{tr}^2\left(\frac{\Delta R}{R_{nom}}\right) + \left(\frac{-\Delta B}{B_{ej}}\right), \text{ since } \frac{dp}{p} = \gamma_{tr}^2\frac{dR}{R} + \frac{dB}{B} \text{ from equation (5.3)}$$

$\Rightarrow$ $\Delta p/p = +1.4\times10^{-4}$ $[\Delta B = +1 \text{ Gauss}]$

6. RF

The tremendous flexibility of the 9.5 MHz ferrite-loaded cavity RF system derives from the fact that, during one cycle, different voltage (and frequency) programmes may be distributed to separate groups of cavities around the machine. The voltage programmes themselves are constructed from a variety of user-dependent functions which modify the basic VRFLE/VRFHE programme according to magnetic cycle type. (The VRFLE and VRFHE voltage programmes are governed by the low- and high-energy working points, respectively.) A hardware matrix performs the mapping of the resultant 'analogue lines' onto specific groups of cavities. This mapping of the six possible analogue lines onto eleven cavities (including one reserve) depends upon harmonic number.

Thus, for the LEA cycle, the programming of $h = 10$ in the PS PLS matrix results in cavities 81, 86, 91 and 96 being supplied with the voltage programme known as analogue line 1, cavities 36 and 46 with analogue line 2 and cavities 51, 56, 66 and 76 with analogue line 3. Analogue line 1 is produced from a fixed combination of several function generators, viz. PA.AFGVRFLE/PA.AFGVRFHE − PA.AFGVREDBU1 − PA.AFGVREDBU2 − PA.AFGVHJ1 − PA.AFGVLM2 − PA.FFGVBC1. It reduces to VRFLE − VREDBU1 − VHJ1, however, when the magnetic cycle type is D, the start timings for the other functions being disabled. Similarly, analogue line 2 is the combination VRFLE − VREDBU1 − VHJ3 and analogue line 3 is VRFLE − VREDBU1 − VHJ1 − VHJ2 for LEA. The voltage reduction function VREDBU1 for the 1 GeV blow-up is, of course, superfluous since it occurs before antiprotons ever enter the machine. It remains by virtue of the similarity which is deliberately maintained between the LEA and TST cycles in order to permit the deceleration of protons. During the normal TST cycle, protons from the Booster are accelerated to 3.5 GeV/c using analogue lines 1, 2 and 3 and they are kept bunched on $h = 20$ by analogue line 2 while the other cavities jump from $h = 20$ to $h = 6 + 12$ prior to ejection towards the AA Complex. During the LEA cycle, cavities 36 and 46 remain on $h = 20$ while the others jump to $h = 10$ prior to the injection of antiprotons from the AA and they are switched off after this harmonic jump by reducing analogue line 2 to zero with the gating function VHJ3. Thus the antiprotons for LEAR are captured and decelerated using only eight PS cavities.

The total detected ($h = 10$) RF voltage during the LEA cycle is shown in Figure 6.1 together with dB/dt. Prior to injection, the voltage is set at a level of ~12 kV (peak), which matches the RF buckets in the PS to the incoming bunch from the AA. 'Matching' prevents quadrupolar synchrotron oscillations and simply means that the phase-space aspect ratio of the buckets is made equal to that of the injected bunch. Thereafter the voltage is increased, first in a parabolic fashion and then linearly, until ~115 kV (peak) is reached before the end of the 3.5 GeV/c ledge. The longitudinal acceptance is now so large that there is no need for the voltage to follow dB/dt during deceleration. However, in order to adapt the bunch in the PS to the RF bucket waiting in LEAR, the voltage is gradually reduced to ~50 kV (peak) before ejection occurs. Immediately after ejection, the RF cavities, having reached the lower limit of their tunable range, are turned off rapidly.

Figure 6.1: Detected (h = 10) RF voltage (channel A) and dB/dt (channel B) triggered at the LEA coarse injection timing, 420 C. (For the first part of the trace, the RF voltage programme mimics the TST proton cycle and the h = 20 voltage is not properly detected.)

The term "adiabatic" is used fairly loosely in accelerator physics to describe anything that happens over a timescale which is long compared with the synchrotron period, τ_s. (This is to be contrasted to its use in thermodynamics, where it applies specifically to processes which involve no energy loss from the system and which are, therefore, very rapid.) The RF voltage manipulations that occur while the LEA beam is in the machine are adiabatic and this has particular consequences just after injection when the voltage is low and the synchrotron period large. We recall the principal parameters of a general RF bucket:

$$\text{Bucket half-height, } H = H_\pi \frac{Y(\sin\phi_s)}{\sqrt{2}} \; ; \; H_\pi = \left[\frac{2eV_{RF}\beta pc}{\pi h|\eta|} \right]^{1/2}$$

$$\text{Longitudinal acceptance} \equiv \text{Bucket area, } S = S_\pi \alpha(\sin\phi_s) \; ; \; S_\pi = \frac{4}{\pi f_{RF}} H_\pi$$

and

$$\text{Synchrotron frequency, } f_s = \frac{1}{\tau_s} = \left[\frac{eV_{RF}\eta\cos\phi_s}{2\pi h\beta pc}\right]^{1/2} f_{RF},$$

where V_{RF} is the peak RF voltage summed over all cavities, ϕ_s is the synchronous phase and where

$$\eta = \frac{1}{\gamma^2} - \frac{1}{\gamma_{tr}^2}$$

In the special case of a stationary bucket (e.g. on the 3.5 GeV/c ledge), $\sin\phi_s = 0$ and the moving-bucket functions become $Y(0) = \sqrt{2}$, $\alpha(0) = 1$, whence

$$f_s = \frac{\pi|\eta|f_{RF}^2}{8\beta pc} S$$

That is,

$$\frac{1}{\tau_s} \propto S \propto V_{RF}^{1/2} \qquad [dB/dt = 0] \qquad (6.1)$$

This is an important result since, in order for the increase in longitudinal acceptance after injection to be adiabatic, the fractional change in bucket area during one synchrotron period,

$$\frac{\Delta S}{S} = \frac{\tau_s}{S}\frac{dS}{dt} \equiv \alpha_c ,$$

must be small. If α_c[1] is too large, the increase in acceptance will be accompanied by an unwanted dilution of the longitudinal phase space density of the beam. It is customary to maintain $\alpha_c < 1$ (typically $0.25 < \alpha_c < 0.50$) and constant so that, integrating over the time interval $[t_0, t_1]$,

$$\alpha_c \int_{t_0}^{t_1} dt = \tau_s(t_0)S(t_0) \int_{S(t_0)}^{S(t_1)} S^{-2} dS \text{ , since } \tau_s S = \tau_s(t_0)S(t_0) = \text{constant from (6.1)}$$

$$\Rightarrow \qquad \alpha_c(t_1 - t_0) = \tau_s(t_0)S(t_0)\left(\frac{1}{S(t_0)} - \frac{1}{S(t_1)}\right)$$

$$\Rightarrow \qquad \frac{S(t_1)}{S(t_0)} = \left(\frac{V_{RF}(t_1)}{V_{RF}(t_0)}\right)^{1/2} = \left[1 - \frac{\alpha_c}{\tau_s(t_0)}(t_1 - t_0)\right]^{-1}$$

[1] An alternative definition of an adiabaticity coefficient is commonly encountered:

$$\alpha_c' = \Omega_s^{-2}\frac{d\Omega_s}{dt} \text{ , with } \Omega_s = \frac{2\pi}{\tau_s} ,$$

which I feel is more contrived. However, it follows from relation (6.1) that $d\Omega_s/\Omega_s = dS/S$ and hence that $\alpha_c = 2\pi\alpha_c'$.

Hence, writing $k = \alpha_c f_1(t_0)$ and $t_0 = 0$, $t_1 = t$,

$$V_{RF}(t) = \frac{V_{RF}(0)}{(1-kt)^2} \tag{6.2}$$

This is the law which governs the RF voltage growth during the first dozen milliseconds after injection. The basic low-energy voltage programme is modified by subtracting the function VHJ2 (see Figure 6.2) which, for the user LEA, is programmed according to equation (6.2).

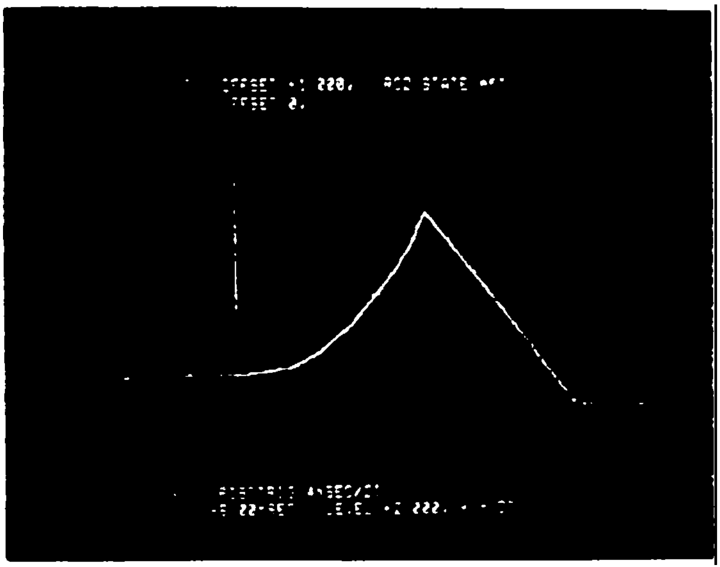

Figure 6.2: The function PA.AFGVHJ2 (displayed inverted) is not used for a harmonic jump during the LEA cycle, instead it affords an adiabatic increase in longitudinal acceptance before deceleration commences. (The oscilloscope is triggered at LEA injection.)

7. TIMING

The structure of the timing for the LEA extraction process is shown schematically in Figure 7.1 together with a complete list of timing values and PLS conditions. The latter may be obtained by running the CPS program (G − D)TIM − LEAR.

The master coarse ejection timing, PX.APLE, is derived from the B-train (strictly, the logical OR of PX.TBU0.1 and PX.TBD0.1) using two general-purpose preset counters in the usual prepulse + pulse-slave configuration. However, since the B-field is falling at ejection, the offset value of the master pulse-slave GPPC (equipment number 4) is negative and appears in 16-bit two's complement form. That is, the direct current control value 64,686 corresponds to − 850, which is the difference

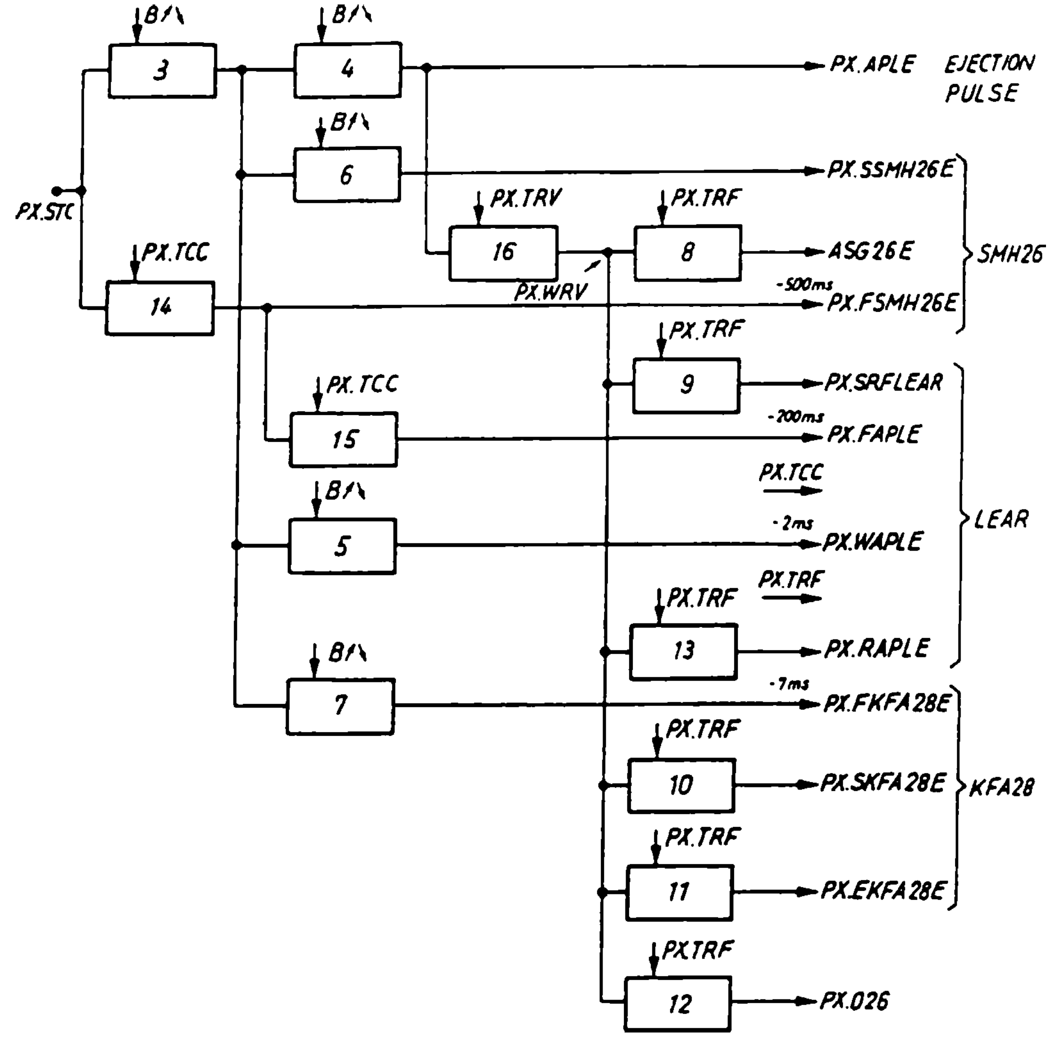

	NAME	EN	CCV	CCVD	AQND	TR	PLS	ENAB	DISAB
1	APLE 1	3	2890	3740	3739	3	14	1	1
2	APLE 2	4	0	64695	64687	5	14	1	1
3	WAPLE	5	47	64733	64734	5	40	1	1
4	SSMH26	6	227	64913	64914	5	14	1	1
5	FKFA28	7	197	64683	64864	5	14	1	1
6	ASG26E	8	1162	1152	1161	4	17	1	1
7	SRFLEA	9	10	10	9	4	40	1	1
8	SKFA28	10	1149	1149	1148	4	14	1	1
9	EKFA28	11	1150	1150	1149	4	14	1	1
10	O26	12	1149	1149	1148	4	14	1	1
11	RAPLE	13	1151	1151	1150	4	40	1	1
12	FSMH26	14	95	95	94	0	14	1	1
13	FAPLE	15	300	300	299	0	40	1	1
14	WRV	16	1	1	0	4	14	1	1

Figure 7.1

between the CCVD and CCV of the master prepulse GPPC (equipment number 3).

Essentially, a GPPC counts clock train pulses and provides an output pulse when the count reaches some specified value. In order to minimize the delay between the arrival of the final clock pulse and the appearance of the output pulse, the comparator of the GPPC tests for the penultimate clock pulse and, when this has been registered, allows the next clock pulse to pass directly to the output. Thus the master prepulse GPPC is programmed, by downloading the value 3,739 B0.1, to fire at 374.0 Gauss as the field rises early in the cycle. The master pulse-slave GPPC, however, counts down (from 374.0 Gauss $\Leftrightarrow 0 \equiv 2^{16}$) during deceleration until the field is 85.0 Gauss lower than this and so $-849 \equiv 64{,}687$ B0.1 is downloaded. The value that is downloaded to a GPPC is the result of a software treatment, so that the corresponding CCVD is correctly adjusted for the ± 1 count and, where applicable, the CCV determines by how much a prepulse is advanced from its master.

The fine timing is, of course, derived from the RF trains. PX.TRV is used to synchronize on the bunch and produce the RF prepulse PX.WRV (equipment number 16), while PX.TRF affords a fine delay for the ejection trigger and acquisition timings.

Ultimately, the LEAR machine itself provides the acid test of the momentum at extraction, but the corresponding field is readily estimated as a control. Assuming that half a turn of the PS is required to synchronize on the antiprotons, taking $f_{RF} \simeq 2.59$ MHz near ejection and neglecting hardware delays, then

$$B_{ej} \simeq B_{PX.APLE} + \left(\frac{PX.SKFA28 + 0.5h}{f_{RF}} \right) \frac{dB}{dt} = 289.0 + \left(\frac{1149 + 5}{2.59 \times 10^6} \right) (-3.05 \times 10^3) = 287.6 \text{ Gauss}$$

This should agree quite closely with the field measured at 595 C, the approximate ejection timing.

Bibliography

The following documentation may prove useful.

J.Boillot, "$\bar{p} \rightarrow$ LEAR" (1987).

J.Philippe, "Layout du timing des injections du PS et de l'ejection LEAR", PS/CO/WP 88-004 (1988).

J.Evans, "The TST cycle", PS/RF/Note 89-2 (1989).

Distribution

OP Engineers
PSS's
OP/PS Section
J. Boucheron
J. Evans
R. Garoby

Distribution (opf abstract)

PS Scientific Staff